Journal of Organometallic Chemistry, 452 (1993) 63–73

JOM 23309

The role of agostic H → Zr interactions in the insertion of olefins with metallocene catalysts. An MO study

Christoph Janiak [1]

BASF AG, Zentralbereich Kunststofflaboratorium – Polyolefine, W-6700 Ludwigshafen (Germany)

(Received September 23, 1992)

Abstract

The possible role of an α-agostic interaction in the course of an olefin insertion at a Ziegler-Natta catalytic centre in $[Cp_2Zr(C_2H_4)CH_3]^+$ has been studied by Extended Hückel calculations. It is shown that in a cationic zirconocene catalyst an α-agostic H → Zr contact plays no role in a ground state species but becomes increasingly important along the reaction coordinate for the C–C bond-forming insertion reaction. This can be traced to the weakening of the $Zr-C_{alkyl}$ bond and the simultaneous transformation to a more electron deficient zirconium species. In contrast, a β-agostic interaction in $[Cp_2Zr(C_2H_4)CH_2CH_3]^+$ leads to a stable ground state β-H → Zr contact. The agostic interaction of *one* hydrogen on the α-carbon is also compared to an agostic contact of *two* α-hydrogens. The behaviour of orbital energies and the H → Zr overlap population has been examined as a function of the angles of methyl tilt and olefin shift.

1. Introduction

During the past decade it has become clear that agostic M ← H–C bonds [1*] (M = metal) can be involved in many aspects of organometallic chemistry, including olefin polymerizations [2,3]. Structural evidence from diffraction experiments suggests the presence of agostic hydrogen(s) on the α-carbon atom (**1**) for a variety of M–alkyl complexes [2,4], in a large class of alkylidene complexes (**2**) of Nb, Ta, and W [2], and in a number of complexes with β-agostic (**3**) or remote (γ, δ, ···) metal ← hydrogen interactions [2,5]. A compound with a β-agostic interaction of special interest to our study is $[(MeC_5H_4)_2(PMe_3)Zr\text{-}CH_2CH_3][BPh_4]$ [6].

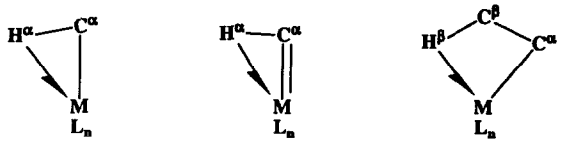

1 2 3

[1] Present address: Institut für Anorganische und Analytische Chemie, Technische Universität Berlin, Straße des 17. Juni 135, D-10623 Berlin (Germany).

* Reference number with an asterisk indicates a note in the list of references.

Along with the experimental studies, the activation of aliphatic C–H bonds in the form of agostic interactions is also attracting great theoretical interest. A variety of calculations deals with the distortions at the α-carbon atom in the ground state geometries of possibly agostic alkyl or alkylidene (carbene) [7] complexes. The alkyl compounds include $(PH_3)_2X_2YTi\text{–}R$ (R = CH_3 [8], C_2H_5 [9,10]; X, Y = H, Cl), $H_5Ti\text{–}R^{2-}$ and $H_3Ti\text{–}R$ (R = CH_3 [11–13], C_2H_5 [12]), $\{(C_5H_5)Fe(CO)\}_2(\mu\text{-}CO)(\mu\text{-}CH_3)$ [14], and $(MCH_3)^+$ fragments [15]. Interestingly an X-α [16] and a Fenske-Hall-MO calculation [17] on $Cl_3Ti\text{–}CH_3$ reveal no distortion on the methyl group and no Ti ← H interaction. Remote agostic interactions have also been investigated [18].

However, the M — H–C interactions in observable ground state geometries represent just the 'tip of the iceberg'. The real importance of agostic interactions lies in their positive role in intermediates and transition states [2,19,20].

For insertion of olefin into a transition metal alkyl bond in Ziegler-Natta polymerization, three basic mechanisms have been suggested, each being supported by experimental evidence: (a) the direct insertion mechanism, proposed by Cossee and Arlman [21], involving a loosely coordinated four-centre transition state; (b) the metathesis mechanism, proposed by Green and Rooney [22], in which an α-hydrogen transfer from

0022-328X/93/$6.00

the end of the polymer chain and formation of a metal carbene/alkylidene precede the formation of a metallocyclobutane complex and (c) the "modified Green-Rooney mechanism" (suggested by Brookhart and Green [2,19]), intermediate between (a) and (b), in which an α-agostic C–H coordination in the transition state assists the insertion of an olefin in a transition metal-catalyzed carbon–carbon bond forming reaction.

In respect of the last mechanism a number of experiments has been designed to explore the suggested role of an α-agostic intermediate in the olefin insertion reaction. Thus while the product of an induced cyclization in racemic 1-d_1-5-hexenyl- and heptenylchlorotitanocene [23] argued against an α-CH activation, the hydrocyclization of *trans,trans*-1,6-d_2-1,5-hexadiene by a scandocene hydride, $Me_2Si(Me_4C_5)_2Sc(PMe_3)H$ [24] as well as the hydrodimerization of (*E*)- or (*Z*)-1-deuterio-1-hexene by achiral zirconocene dichloride/methyl alumoxane (MAO) [25] gave results judged to provide experimental evidence for an α-agostic transition state (modified Green-Rooney mechanism) in metal-catalyzed olefin polymerizations.

Some theoretical studies on the mechanism in Ziegler-Natta polymerizations investigated the possibility of agostic interactions. Jolly and Marynick [26] used the model system '$Cp_2Ti{-}CH_3^+ + C_2H_4 \rightarrow Cp_2Ti{-}C_3H_7^+$' and concluded that the direct insertion mechanism (Cossee-Arlman) is viable even without agostic interactions. However, a study by Kawamura-Kuribayashi *et al.* [27] on '$Cl_2Ti{-}CH_3^+ + C_2H_4 \rightarrow Cl_2Ti{-}C_3H_7^+$' found strong agostic interactions. Prosenc *et al.* also favoured α-agostic stabilization of the transition state during insertion of an α-olefin into a zirconocene alkyl cation [28].

Our objective is to throw light on the electronic features in possible agostic interactions along a reaction coordinate for an olefin insertion. These studies form part of our programme to develop a deeper understanding of Ziegler-Natta catalysis with the help of homogeneous, soluble, molecular-defined titanocene and especially zirconocene-methylalumoxane systems (these metallocenes are also regarded as constituting a new generation of industrial olefin-polymerization catalysts [29]).

Using zirconium model complexes in our theoretical study we aim at increasing understanding on the basis of a qualitative molecular orbital picture within the Extended Hückel formalism. Extended Hückel theory is a very transparent method allowing us to develop an understanding of the orbital interactions, *i.e.* the electronic interactions involved in such an M ← H contact. Such orbital interactions between the central metal and its ligands are at the core of our study. What distinguishes this approach from others is that it focusses less on the distortions in the M–C bond and more on the M ← H–C interaction.

"Steric" ligand–ligand interactions (such as M–$CH_2R \leftrightarrow Cp'$, $H_2C{=}CHR \leftrightarrow Cp'$) are also not explicitly considered here. Such interactions probably play the dominant role in determining the stereochemistry of a polypropylene polymer, especially in connection with chiral substituted Cp's [30], but such a study of "steric" interactions is better left to molecular mechanics calculations [31]. Therefore, we can restrict ourselves to methyl as representing the growing alkyl chain, to ethylene as the olefin, and to normal cyclopentadienyl ligands for the metallocene moiety. It is unnecessary to look at propylene insertion and chiral metallocene systems for the purpose of this study.

1.1. The reference system

In light of the smallness of the agostic effect the availability of a suitable reference system appears essential to decide what role, if any, the H → Zr agostic interaction plays in the Zr–C bond distortion and olefin insertion process. The reference system needed is one exhibiting no agostic interaction but with all other geometrical parameters as close as possible, preferably even identical.

The only suitable reference values are obtained by deleting the overlap matrix element S_{ij} between all (or selected) orbitals on the agostic H and Zr atoms. A deletion of all orbital overlaps is, of course, equivalent to an overlap deletion between the atoms. Setting all $S_{H,Zr}$ equal to zero allows the calculation of geometrically exactly the same molecule with and without the agostic interaction. Setting certain S_{ij} at zero will affect everything from the orbital and total energy to orbital composition and overlap populations [32,33]. Orbital energies and overlap populations are the descriptors we will use mostly, to develop a deeper understanding of the agostic interaction.

There are, of course, a number of assumptions involved in our model- and reaction coordinate set-up. We assume that the methyl (or alkyl) and olefin fragment approach each other in the "equatorial" plane between the cyclopentadienyl (or any other) ligands (the paper plane in **4**), so that C_s-symmetry is preserved during the reaction. The olefin also lies within this plane (not perpendicular to it). We also assume that the methyl-C_3 axis will tilt to make way for the incoming olefin, thus minimizing repulsion, and that

this methyl tilt (γ) can be separated from the movement of the olefin (δ-shift). These geometric variations are illustrated in **4**.

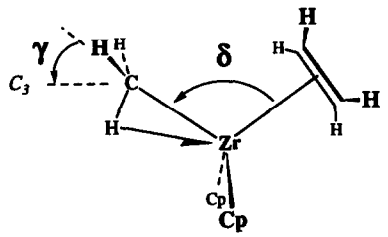

4

For the sake of simplifying our theoretical investigation, we preserve the local geometry of the methyl group (C_{3v}) and the olefin, *i.e.* keep C–H distances and H–C–H angles constant. The olefin fragment is bonded symmetrically to the zirconium with the hydrogens bent back by 20°, a well documented effect in such metal-π complexes [34]. The distances for all (chemically) bonded contacts will remain constant. The basic Extended Hückel method is known not to give reliable distances [33], and this precludes variation of the distance in our calculations. The geometrical parameters used are given in the Appendix.

2. Results and discussion

We present a molecular orbital analysis for the methyl tilt and olefin shift in the system $[Cp_2Zr(C_2H_4)CH_3]^+$ (**4**). Figures 1 and 2 show the Walsh diagrams for these geometric changes in $[Cp_2Zr(C_2H_4)CH_3]^+$. Despite their complicated appearance we have analyzed these Walsh diagrams in full detail. However, we prefer to present most of our results with the help of the model complexes **5** and **6**, in which the cyclopentadienyl ligands (and the ethylene fragment) have been replaced by hydrogens.

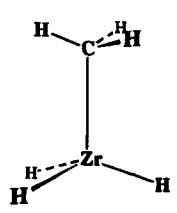

5

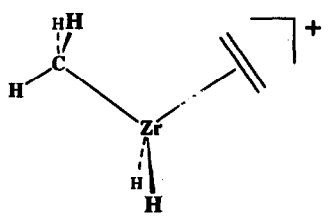

6

Replacing a large complicated group by a simpler ligand is a standard operation to simplify theoretical calculations and presentations. Although the shift from a cyclopentadienyl ligand to a hydrogen may seem rather drastic, it does not, in fact, alter the essential electronic features we are about to discuss, but allows us to point them more clearly [36]. We should emphasize, though, that it is the complex $[Cp_2Zr(C_2H_4)CH_3]^+$ that has been analyzed and the sole purpose of using **5** and **6** is to present our findings more concisely.

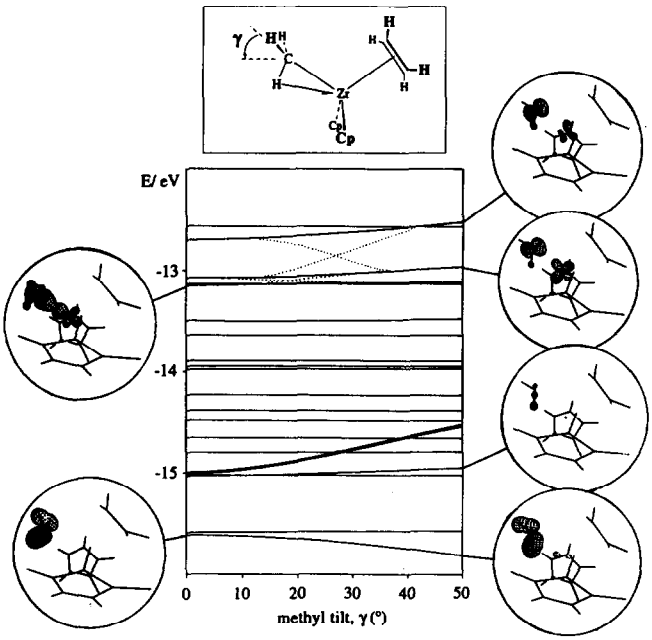

Fig. 1. Partial Walsh diagram for the methyl tilt (γ) in $[Cp_2Zr(C_2H_4)CH_3]^+$ (**4**). Important orbitals are shown as CACAO plots [35], with only the CH_3 and Zr contributions shown for clarity; the dotted lines depict some orbital level mixings/avoided crossings. The total energy is shown as the thick curve and scaled to the energy of the orbital levels.

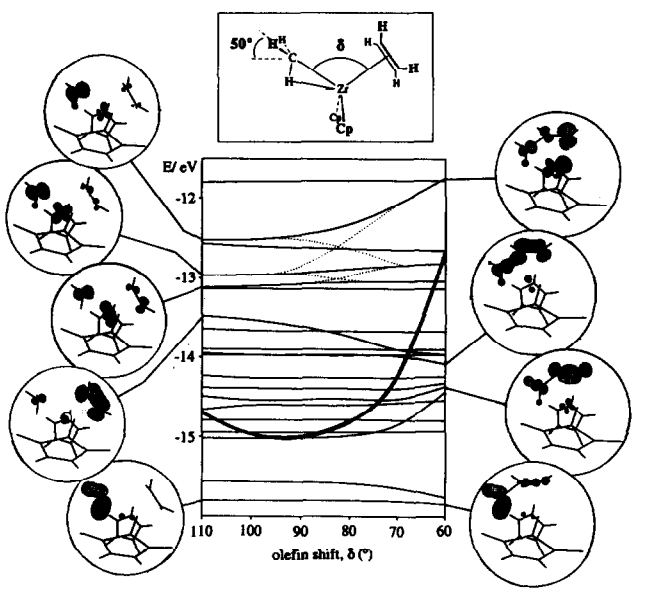

Fig. 2. Partial Walsh diagram for the olefin shift (δ) in $[Cp_2Zr(C_2H_4)CH_3]^+$ (**4**). Important orbitals are shown as CACAO plots [35] with only the CH_3, Zr and C_2H_4 contributions shown for clarity; dotted lines depict some orbital level mixings/avoided crossings. The total energy is shown by the thick curve and scaled to the energy of the orbital levels.

2.1. The methyl tilt

2.1.1. C–Zr Bond distortion in $L_3Zr–CH_3$

The tilting of the methyl group has already been analyzed by others [11,13,15] and can be summarized as follows: the total energy closely parallels the energy variation of the Zr–C σ-bond localized in the HOMO. the increase in energy as CH_3 is tilted can be traced to a decrease in overlap, and hence in bonding interaction between the Zr $-z^2$ and the $n(CH_3)$ orbital (we use the notation $z^2 \equiv d_{z^2}$). This is depicted in **7**. The decrease is only partially compensated by an increase of overlap to other Zr-orbitals lying in the xz-plane (sketched in **8a** and **b**), the interaction with the energetically closer orbital shown in **8a** being the dominant one.

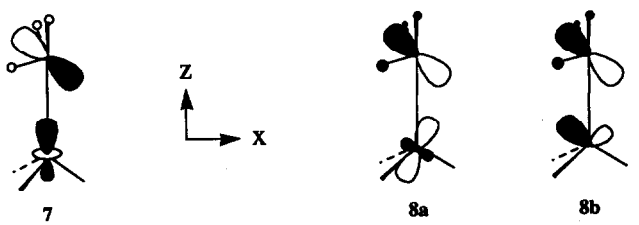

7 **8a** **8b**

2.1.2. The α-agostic hydrogen–zirconium interaction

The agostic C–H → Zr interaction increases as the H → Zr distance becomes smaller, with tilting of the methyl group, as discussed in the preceding section. To evaluate the energetic contribution of the H → Zr overlap, we examined the orbital energies and orbital overlaps for the C–Zr and H → Zr bonding orbitals as a function of tilt angle. What is refered to here and below as the H → Zr "bonding orbital" is, of course, primarily the Zr-s–H_3 or Zr-s–(ligand)$_3$ bonding combination, especially so in the undistorted case. Upon distortion there is a larger and larger C–H$^\alpha$ contribution to this level from a CH_3 combination of the same symmetry (in the tilted structure) in an orbital lying above.

Figure 3 shows a partial Walsh diagram for the methyl tilting in **5**. As in Fig. 1, the H → Zr level (1a′, C_s symmetry) is slightly lowered in energy, while the C–Zr orbital (here HOMO) is raised. The sum of both energy changes matches the variation in the total energy (see insert). From this it appears as if though the agostic H → Zr interaction has only a stabilizing effect.

However, the situation is not this simple. If we make a comparison with the energetic changes for $S_{H,Zr} = 0$ for both orbitals (dashed lines), we see that 1a′ (previously the H → Zr level)–is unaffected by the angle variation, while the C–Zr orbital experiences an overall lowering in energy and a smaller increase upon distortion (Fig. 3). The latter effect is due to a destabilizing H → Zr contribution to the C–Zr bonding orbital

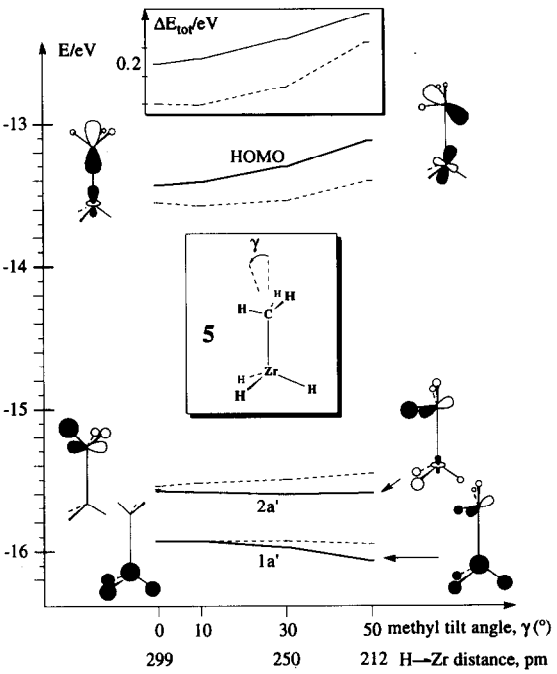

Fig. 3. Partial Walsh diagram for the methyl tilt (γ) in $H_3Zr–CH_3$ (**5**). Only important orbitals are given; dashed lines are for $S_H\alpha_{,Zr} = 0$. The curve for the total energy is given at the top of the diagram. Setting the agostic hydrogen-zirconium overlap to zero leads to a lower energy of the HOMO and a smaller increase upon tilting, indicating a destabilizing H → Zr contribution to this orbital. The orbital representations are schematic (compare with Fig. 1); symmetry labels for C_S.

that can be traced to a small hydrogen contribution to the HOMO which gives rise to an antibonding H → Zr interaction. This antibonding H → Zr contribution can be more clearly seen from a plot of the H → Zr orbital overlap population as a function of tilt angle, shown in Fig. 4. The HOMO, already H → Zr antibonding in the undistorted structure, attains a somewhat more negative H → Zr overlap population as a result of methyl tilting. Even so, as the hydrogen and zirconium come closer together, their total overlap population (bold line) increases strongly, the curvature being largely determined by the 1a′ and 2a′ orbitals. This strong increase may indicate increasing importance of the agostic interaction along the reaction coordinate.

Please note that the 1a′ and the 2a′ level are of different symmetry at $\gamma = 0°$ (point group C_{3v}) hence their mixing is forbidden at this angle. However, as soon as methyl tilting causes symmetry lowering, they will mix.

2.2. The C_{methyl}–C_{olefin} bond forming reaction, the olefin shift (δ)

We now decrease the C_{methyl}–Zr–$C_{(ethylene\ centre)}$ angle, δ, to a fixed methyl tilt angle of, say, $\gamma = 50°$, so as to approach the potential transition state for formation

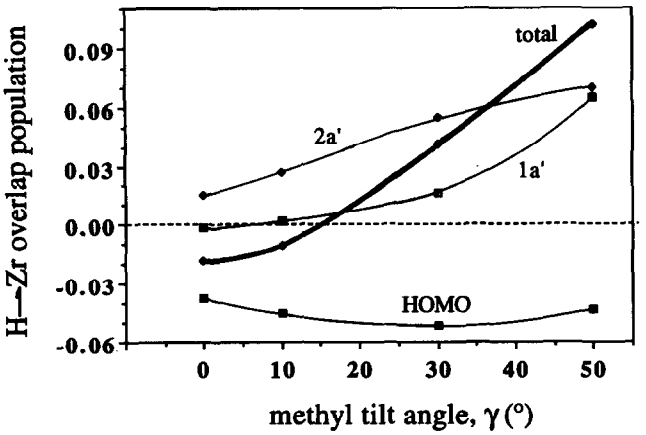

Fig. 4. The agostic hydrogen-zirconium overlap population as a function of methyl tilt (γ) in $H_3Zr{-}CH_3$ (**5**). An orbital-by-orbital breakdown of the total overlap population (bold curve) has been carried out, and major contributions from the 1a', 2a' orbital and the HOMO are included (*cf.* Fig. 3). Note the strongly H → Zr antibonding character of the HOMO.

of the C_{methyl}–C_{olefin} bond. This δ variation is carried out in such a way that only the olefin moves, with the position of the methyl group kept fixed.

As the angle δ is decreased from 110° and one end of the ethylene approaches the methyl group, the total α-agostic H → Zr overlap population continues to increase further (see Fig. 5), even though the H → Zr distance is kept constant. This indicates the increasing importance of the agostic interaction along the reaction coordinate. The increase in H → Zr overlap population is mainly due to a change in character of the HOMO from something of a H → Zr "antibonding" to

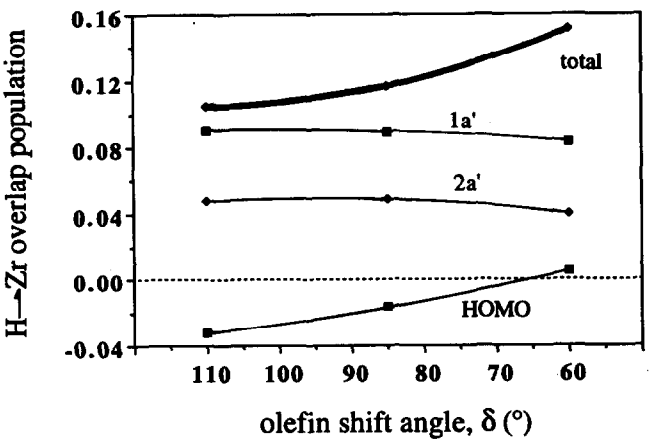

Fig. 5. The change in agostic hydrogen-zirconium overlap population with the olefin shift (δ) in $[H_2Zr(C_2H_4)CH_3]^+$ (**6**). Note the further increase of the total H → Zr overlap population (bold curve) as the ethylene fragment approaches the methyl group (δ gets smaller) owing to a change of the HOMO character from H → Zr anti- to nonbonding.

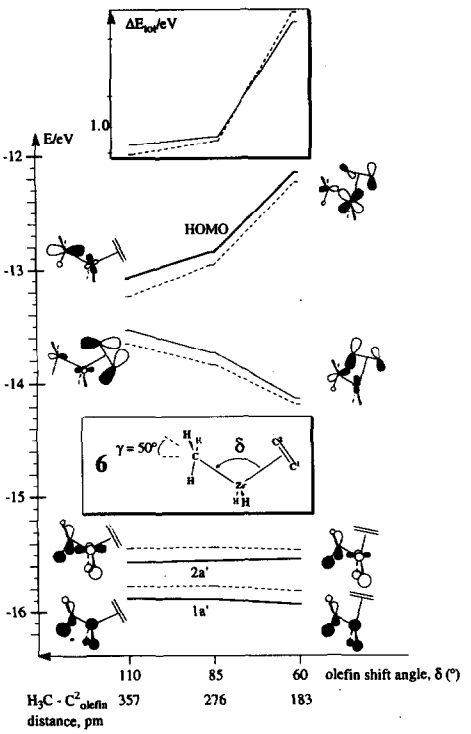

Fig. 6. Partial Walsh diagram for the olefin shift (δ), *i.e.* the approach of the ethylene to the methyl fragment in $[H_2Zr(C_2H_4)CH_3]^+$ (**6**). Only important levels are shown; dashed curves are for $S_{H\alpha,Zr} = 0$; orbital representations are schematic (compare to Fig. 2); symmetry labels for C_s.

a "nonbonding" level. The HOMO that is still increasing in energy undergoes a change in Zr composition due to orbital mixing (see sketches in Fig. 6).

Another indication of more dominant influence of the agostic interaction as the transition state is approached comes from a comparison between the total energies for complexes with "normal" $S_{H,Zr}$ and with $S_{H,Zr} = 0$ (overlap deleted). The energy difference between the total energies for normal and zero $S_{H,Zr}$-overlap matrix elements decreases as the methyl tilt angle becomes larger than 30° (*cf.* insert in Fig. 3). This trend continues in Fig. 6 with a decrease in the δ-angle, and leads to a curve crossing. With the curves crossing each other the agostic complex becomes energetically more favourable than the non-agostic reference system; in other words, the agostic H → Zr interaction represents a stabilizing element as the methyl and ethylene fragment approach each other and the new C–C bond is formed. This behaviour of the total energies is a consequence of the orbital energies for the HOMO and HOMO-1.

It must be remembered that the features presented above with the help of the model system **5** and **6** actually present the results of an MO analysis for the $[Cp_2Zr(C_2H_4)CH_3]^+$ complex. It can be clearly seen

that the important orbital level changes in Figs. 3 and 6 correspond to the changes in Figs. 1 and 2, respectively, but without perturbation by avoided crossings.

The increasing relevance of an agostic interaction towards and beyond the transition state can be understood in terms of a change from a (formally) 16-electron $[Cp_2Zr(C_2H_4)CH_3]^+$ to a 14-electron $[Cp_2Zr\text{-}CH_2CH_2CH_3]^+$ system as the olefin undergoes insertion into the Zr–C bond. In the absence of other stabilizing ligands the product is highly electron deficient, and thus needs some agostic stabilization before the next olefin enters the coordination sphere. We can artificially increase the electron deficiency and thereby elucidate this phenomenon in more detail.

We carried out a calculation in which the Zr–C overlap was set to zero in $H_3Zr\text{–}CH_3$. This leaves the Zr centre with one electron less than before with normal $S_{Zr,C}$ values. In Fig. 7 the results for the model complex **5** with $S_{Zr,C}\alpha = 0$ (right half) are contrasted with our earlier results for **4** with "normal" S_{ij} values (left half, *cf.* Fig. 3), showing the important orbital energies as a function of the methyl tilt angle.

For **5** with no Zr–C bond, the energy of the HOMO and, thus the total energy of the complex, decreases with γ, in contrast to the results with the Zr–C bond present, for which we found that the agostic overlap contributed in part to the destabilization of the HOMO.

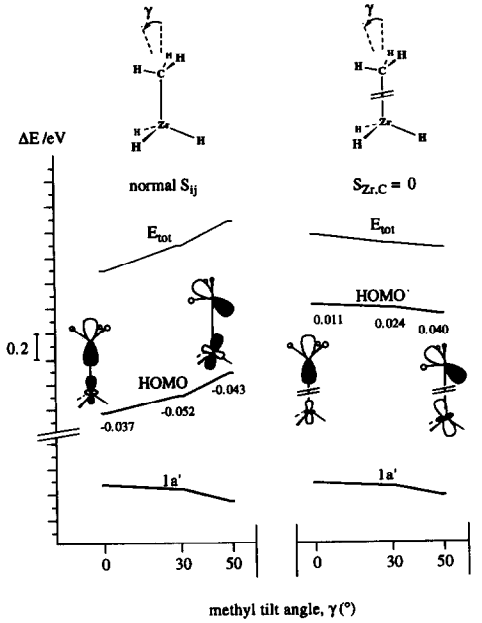

Fig. 7. A comparison of partial Walsh diagrams for the methyl tilt in $H_3Zr\text{-}CH_3$ (**5**) with normal S_{ij} values (left half) and with $S_{Zr,C} = 0$ (right half). Note the stabilization of the HOMO with γ for the latter. Removing the Zr–C interaction induces an electron deficiency at the zirconium. The numbers on the curve for the HOMO correspond to the H–Zr overlap populations at various tilt angles.

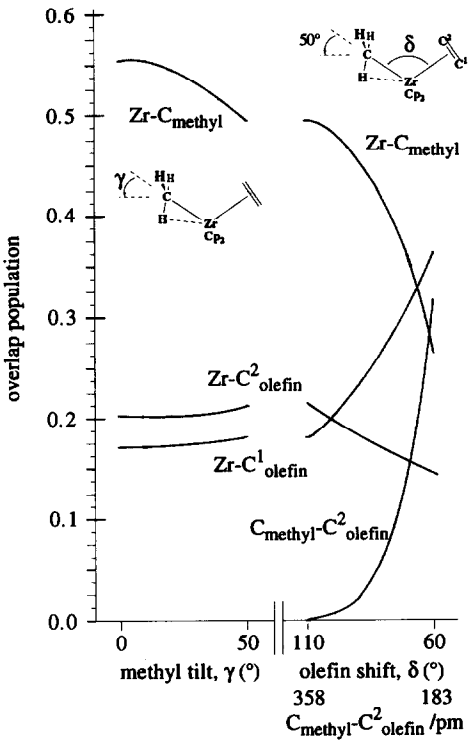

Fig. 8. Variation in the overlap populations of the zirconium-carbon bonds with the methyl tilt angle, γ (left half) and the olefin shift angle, δ (right half) in $[Cp_2Zr(C_2H_4)CH_3]^+$ (**4**). For the change in δ-angle, *i.e.* the approach of the olefin and methyl fragment, the change in the C_{methyl}–C^2_{olefin} bond strength, measured by its overlap population, is also included. Note the strengthening of the Zr–C^1_{olefin} bond, the weakening of Zr–C^2_{olefin} and the drastic loss in bond strength for Zr–C_{methyl} as the transition state of the C–C bond forming process is approached (δ-variation, right half).

The loss of a ligand, along with the electron deficiency it induced on the Zr centre, which has been simulated here, illustrates the critical need of, and susceptibility of the system to, some additional stabilization through agostic interactions.

The absence of a Zr–C_{methyl} interaction is only an extreme case of a weakened Zr–C bond, and the strengthening of the H → Zr interaction correlates with a weakening of the Zr–C_{methyl} bond as the new C_{methyl}–C_{olefin} bond is formed. Thus, it seemed appropriate to carry out an investigation of the Zr–C_{methyl} and Zr–C_{olefin} overlap populations as a function of methyl tilt and olefin shift in $[Cp_2Zr(C_2H_4)CH_3]^+$.

2.3. The development of the Zr–C bonds in the course of the olefin insertion process

Figure 8 shows the variation in Zr–C_{methyl}, Zr–$C^{1,2}_{olefin}$, and C_{methyl}–C^2_{olefin} overlap population as a function of the methyl tilt angle, γ, and the olefin shift angle, δ, for (**4**).

Tilting the methyl group lowers the Zr–C_{methyl} overlap population only slightly (left half of Fig. 8). It is the

approach of the ethylene to the methyl fragment that gives rise to major changes in the overlap populations (right half of Fig. 8). Within the Extended Hückel formalism, the $Zr-C_{methyl}$ and $Zr-C_{olefin}$ bond lengths were kept fixed during the course of our angle variations and both $Zr-C^{1,2}_{olefin}$ contacts taken as equal. In a synergistic process a change in overlap populations can, of course, be assumed to coincide with a change in bond length, a decrease in the population being accompanied by an increase in bond length. The effect of one Zr–C bond becoming longer than the other should, however, become clearer if both bonds are kept fixed and equal.

Figure 8 shows that both $Zr-C^{1,2}_{olefin}$ contacts in $[Cp_2Zr(C_2H_4)CH_3]^+$ start out with a similar overlap population in the pseudotetrahedral complex geometry. Upon distortion of the δ-angle, however, the $Zr-C^1$ bond is strengthened and the $Zr-C^2$ bond weakened, the difference being quite large even for a still rather long and weak $C_{methyl}-C_{olefin}$ interaction. The $Zr-C_{methyl}$ overlap population is lowered considerably, and it is this induced weakening of the $Zr-C_{methyl}$ bond, and the corresponding inherent increase in electron deficiency at Zr, which allows the H → Zr interaction to play a more dominant role around and beyond the transition state.

The behaviour of the Zr–C overlap populations, and corresponding Zr–C bond lengths, is in accordance with the general assumptions for the bonding mechanism of an olefin insertion depicted in **9**.

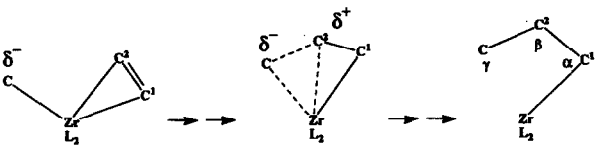

9

We note that the α-agostic stabilization with which we started is transformed into a γ-agostic interaction in the insertion product. The electronics of such a γ-stabilization are very similar to that of a β-agostic interaction, discussed below.

2.4. The 'double' α-agostic interaction

So far we have considered an α-agostic interaction with only one hydrogen from the methyl (or more generally any alkyl group) in contact with the zirconium centre, and we refer to this as a 'single' agostic interaction. It is possible, however, to envisage a different α-agostic mode in which two hydrogens interact simultaneously with the metal as depicted in **10**.

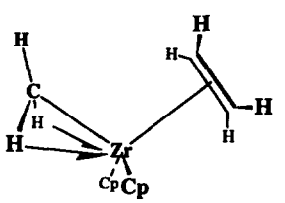

10

The difference between a 'single' and 'double' α-agostic interaction extends beyond the H → Zr contact: In a 'single' α-agostic contact, the remaining two hydrogens of the methyl group are eclipsed with respect to the approaching C–H bonds of the ethylene (see **4**). In a 'double' α-agostic mode, however, the third methyl C–H bond is staggered with respect to the C–H bonds of the ethylene ligand (see **10**).

The Walsh diagram for the methyl tilt in **10**, shown in Fig. 9, together with the overlap populations as a function of methyl tilt angle (not shown), reveals that 'single'- and 'double' agostic interaction are qualitatively electronically rather similar (compare to Fig. 1). A difference is that antisymmetric zirconium orbitals are now able to interact with a π-type hydrogen combination, giving rise to an additional antisymmetric bonding level. No electronic preference can be discerned for either agostic interaction on the basis of methyl tilting and the H → Zr interaction(s) alone. However, the total energy (included in Fig. 9) rises much more upon methyl tilting in **10** than for the 'single' agostic interaction with the comparable complex **4**. This difference in energetic behaviour can be traced to a more pro-

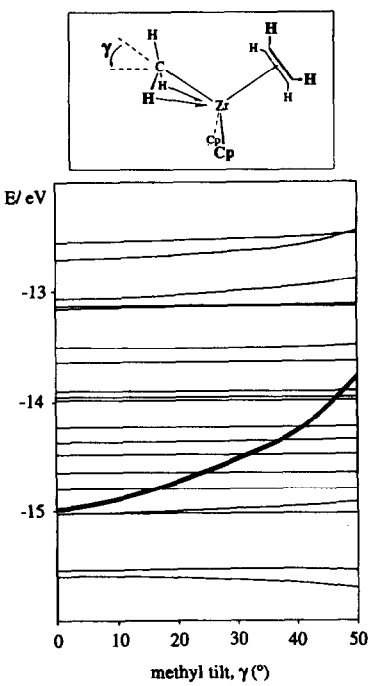

Fig. 9. Partial Walsh diagram for the methyl tilt (γ) in **10** giving rise to a double agostic interaction. Note the similarity in the orbital level energies to the single agostic mode (**4**, Fig. 1) but the stronger increase in total energy (bold curve).

nounced "steric" H_{methyl}–H/C_{Cp} interaction in **10**, which will be even more dominant when substituted cyclopentadienyl ligands are used.

2.5. β-Agostic interaction

We now come to β-agostic interactions, whose importance extends far beyond the simple α/β theoretical comparison within the scope of this article. β-Agostic interactions play an important role in chain termination in the polymerization with metallocene catalysts; the β-hydride elimination (**11**) is recognized as the main termination mechanism, affording polymers with a terminal double bond. Furthermore, β-hydride elimination is also responsible for the instability of many transition-metal alkyl complexes.

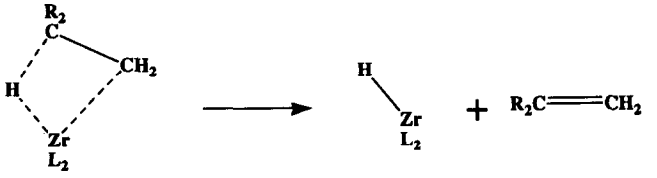

11

In the light of this knowledge, we expect that a β-agostic interaction will be of a different quality than α. We expected, without having carried out calculations, that a β-agostic interaction would tend to be a more *exothermic* bond forming process, leading to a hydrogen–metal contact in an observable, ground state species. Such is the case in the complex $[(MeC_5H_4)_2Zr(PMe_3)CH_2CH_3]^+$, as revealed by an X-ray structural investigation [6], and in the related compounds $[(MeC_5H_4)_2Zr(PMe_3)CH_2CH_2R]^+$ (R = Et, $SiMe_3$, and Ph) as indicated by NMR data. Our calculations should be able to reproduce this observation, and thereby increase our confidence in the α-agostic results.

To understand the basic electronics of the $H^\beta \rightarrow Zr$ interaction and to pinpoint any changes from the α-agostic case we analyzed the complex $[Cp_2Zr(C_2H_4)CH_2CH_3]^+$. However, for reasons given above our findings can again be better illustrated with **12** as a simple model complex.

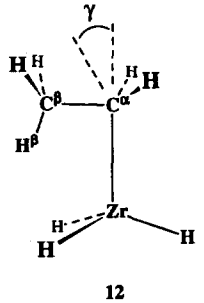

12

Tilting the *methylene* group moves the hydrogens on the *methyl* group (here H^β) closer to the zirconium.

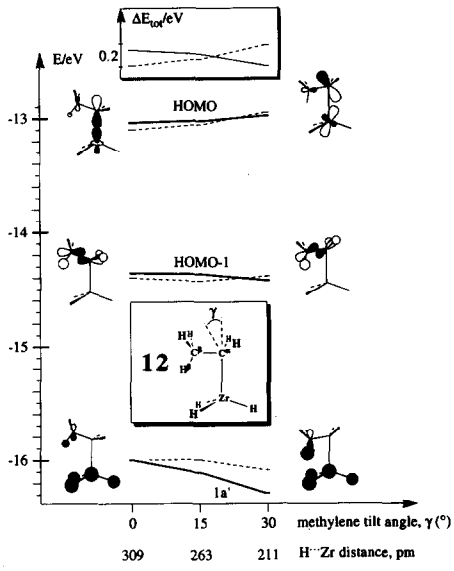

Fig. 10. Partial Walsh diagram for the methylene tilt (γ) in H_3Zr–CH_2CH_3 (**12**), giving rise to a β-agostic H–Zr interaction. Only important orbital curves are drawn; dashed lines are for $S_{H\beta,Zr} = 0$. The curves for the total energies are given at the top. Note the increase in total energy for the zero H^β–Zr overlap with γ and the large H^β contribution to the HOMO-1. The orbital representations are schematic.

The results of this methylene tilt are graphically represented in Figs. 10 and 11. From the Walsh diagram for **12** in Fig. 10 we see clearly the exothermic character of the β-agostic interaction. The curves for the total energy (inserted at the top in Fig. 10) and total overlap

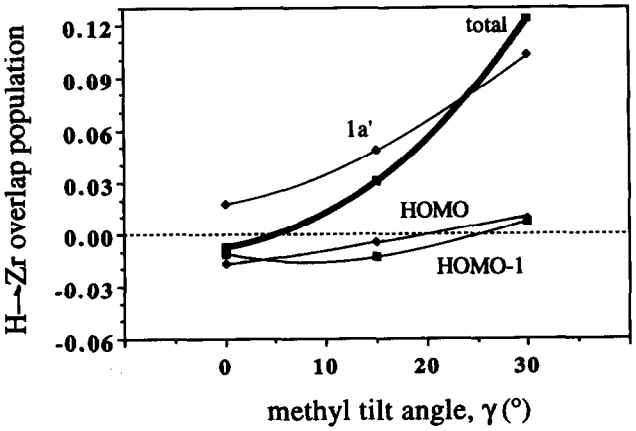

Fig. 11. The β-agostic hydrogen-zirconium overlap population as a function of methylene tilt angle in H_3Zr–CH_2CH_3 (**12**). An orbital-by-orbital decomposition of the total overlap population (bold curve) has been carried out and major contributions from the 1a′ orbital, the HOMO and HOMO-1 are included. Note the essentially H–Zr nonbonding character of the HOMO when compared with the α-agostic methyl tilt in **5** (see Fig. 4; the vertical scale has been expanded to more negative values to allow a better comparison with Fig. 4).

population (Fig. 11) are dominated by the major H → Zr bonding contributor, the 1a′ orbital. Setting $S_H\beta_{,Zr} = 0$ for **12** reverses the stabilizing trend just noted. We point out that a β-interaction allows the same H → Zr distance as observed for α in the model complex **5** to be reached at a smaller tilt angle.

By comparison with the α-agostic interaction in **5** (Fig. 3, 4) we can trace this exothermic β-interaction not to a stronger H → Zr overlap population contribution from the 1a′ orbital in the latter but to the H^β → Zr non-bonding character of the HOMO. This variation in the HOMO character constitutes *the* essential difference between a β- and an α-agostic interaction.

The non-bonding feature of the HOMO for β can be understood from the orbital sketches in Fig. 10, together with our findings of the crucial role of the C^α–Zr bond strength and variation for the H^α → Zr interaction. The Walsh diagram for the β-agostic interaction indicates that the HOMO is again the Zr–C^α bonding orbital, but with only a negligible β-hydrogen contribution. Within the frontier levels the major β-hydrogen component is on the HOMO-1 (the orbital directly below the HOMO), a predominantly C^α–C^β bonding orbital, which on the other hand has almost no zirconium contribution. Therefore, the C^α methylene tilt has a much smaller effect on the H^β → Zr interaction in the HOMO compared with that of the methyl tilt in the α-agostic case.

The question arises of why a β agostic interaction such as depicted in **13** should not be much better suited to play a role in an olefin insertion process. The answer can again be found in steric interactions. The energy for the olefin shift (δ variation)

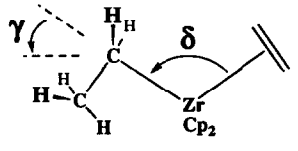

13

rises much more in the β case than the α. This is due to a stronger $H_{alkyl} \cdots H_{olefin}$ repulsion, since the methylene group cannot be tilted as much as in the α agostic interaction. A repulsive $C\text{–}H^\beta_{alkyl} \cdots C\text{–}H_{Cp}$ interaction with the bulky cyclopentadienyl groups develops rapidly with the methylene tilting in our geometrical set-up for **13**, and severely limits the feasible methylene tilt angle, γ. We enter here, of course, a region which is better dealt with by molecular mechanics calculations [31]. The steric $C\text{–}H^\beta \cdots Cp$ interactions depend, of course, on the position of the C^α carbon in the zirconium coordination sphere.

The X-ray structure of $[(MeC_5H_4)_2Zr(PMe_3)CH_2\text{-}CH_3]^+$ [6] revealed an H^β → Zr contact of 216 pm and a methylene tilt angle of a little less than 30° (Zr–C^α–C^β = 83.0 or 84.7°; two independent molecules in the unit cell), and showed that Zr–C^α deviates only by an estimated 10–20° from the maximum opening of the Cp-ring planes. If we imagine the PMe_3 ligand to be replaced by an olefin in this structurally studied complex, we are still left with the repulsive $C\text{–}H_2^\alpha \cdots H_2C{=}CH_2$ overlap because of the small methylene tilt, and we feel that these steric interactions cast doubt on a suggested role for a β-hydrogen → zirconium overlap [6] during the course of the C_{alkyl}–C_{olefin} bond forming reaction with metallocene catalysts.

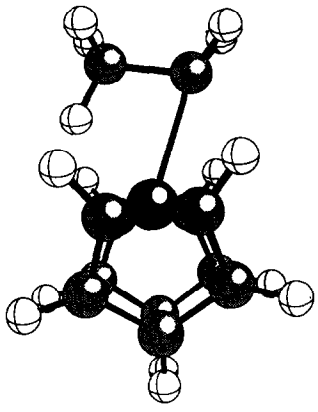

14

Consequently, a β-hydride elimination as the competing reaction for the olefin insertion is likely to take place with no olefin or only smaller ligands present in the coordination sphere of the central metal. This then allows the H^β → Zr contact to develop in the opening created by the cyclopentadienyl ring planes, as depicted in **14**.

3. Conclusions

We can summarize the findings of this analysis of the overlap populations and energies for the H → Zr interaction as follows:

(a) the α-agostic interaction is unimportant in the ground state of the possible catalytic $[Cp_2Zr(C_2H_4)CH_3]^+$ complex. An antibonding H^α → Zr overlap in the HOMO adds a destabilizing component to the C_{methyl} tilt;

(b) the strong antibonding H^α → Zr overlap in the HOMO is overcome only through a Zr–C_{methyl} bond weakening in the course of the C_{methyl}–C_{olefin} approach, *i.e.* the bond forming reaction. In other words, the α-agostic stabilization becomes important only

through an increase in electron deficiency of the central metal, in this case, the gradual transformation of a formally 16e$^-$ $[Cp_2Zr(C_2H_4)CH_3]^+$ to a 14e$^-$ $[Cp_2Zr\text{-}CH_2CH_2CH_3]^+$ zirconium centre. Hence, the calculations strongly support the presence of an α-agostic H → Zr interaction around and beyond the transition state for the olefin insertion (modified Green-Rooney mechanism);

(c) the expected non-symmetric binding of the olefin fragment is revealed clearly by our calculation on $[Cp_2Zr(C_2H_4)CH_3]^+$ as the olefin and methyl fragment approach each other and the new C–C bond is formed;

(d) We cannot see any electronic preference for an α-agostic interaction represented by one in-plane hydrogen ('single'-mode) or two out-of-plane hydrogens ('double'-mode). The latter can, however, be excluded for steric reasons ($H^\alpha \cdots CH_{Cp}$ repulsion);

(e) A β-agostic interaction, on the other hand, is shown by the calculations to be a stabilizing feature in the ground state of $[L_2Zr(C_2H_4)CH_2CH_3]^+$ (L = H, Cp) model complexes. This difference between the α and β interactions can be attributed to the negligible admixture of an H^β contribution to the $Zr\text{–}C^\alpha$ bonding orbital, thus avoiding a strongly antibonding H^β → Zr overlap. We are doubtful, however, that a β-agostic interaction plays a role during the olefin insertion reaction in view of the strong steric $H^\alpha \cdots (H\text{–}C)_{olefin}$ and $(C\text{–}H)^\beta \cdots (C\text{–}H)_{Cp}$ repulsion associated with the geometrical requirements of such a β-agostic interaction.

Acknowledgments

The work was initiated during a postdoctoral stay at BASF AG, Ludwigshafen (Germany). I gratefully acknowledge the award of a BASF-stipend and current support by a DFG-Habilitation Fellowship. Mr. M.-H. Prosenc and Prof. H.-H. Brintzinger are thanked for helpful discussions. I wish to express my gratitude for donations from the 'Fonds der Chemischen Industrie' and the 'Freunde der TU Berlin'. I thank Dr. D.M. Proserpio for making available a copy of the CACAO-program.

References and notes

1 The half-arrow convention, suggested by Brookhart *et al.* [2], is used here as a representation of agostic bonds. The style A · · · B description is used to indicate a chemical bond, weaker than a "normal" or stronger A–B bond.

2 M. Brookhart, M. L. H. Green and L.-L. Wong, *Prog. Inorg. Chem., 36* (1988) 1.

3 K. Mashima and A. Nakamura, *J. Organomet. Chem., 428* (1992) 49.

4 Z. Dawoodi, M. L. H. Green, V. S. B. Mtetwa and K. Prout, *J. Chem. Soc., Chem. Commun.*, (1982) 1410; Z. Dawoodi, M. L. H. Green, V. S. B. Mtetwa, K. Prout, A. J. Schultz, J. M. Williams and T. F. Koetzle, *J. Chem. Soc., Dalton Trans.*, (1986) 1629; A. Barry, Z. Dawoodi, A. E. Derome, J. M. Dickenson, A. J. Downs, J. C. Green, M. L. H. Green, P. M. Hare, M. P. Payne, D. W. H. Rankin and H. E. Robertson, *J. Chem. Soc., Chem. Commun.*, (1986) 520; J. Z. Cayias, E. A. Babaian, D. C. Hrmcir, S. G. Bott and J. L. Atwood, *J. Chem. Soc., Dalton Trans.*, (1986) 2743; K. H. den Haan, L. J. de Boer, J. H. Teuben, A. L. Spek, B. Kojic-Prodic, G. H. Hays and R. Huis, *Organometallics, 5* (1986) 1726; G. Jeske, H. Lauke, H. Mauermann, P. N. Swepston, H. Schumann and T. J. Marks, *J. Am. Chem. Soc., 107* (1985) 8091; J. W. Bruno, G. M. Smith, T. J. Marks, C. K. Fair, A. J. Schultz and J. M. Williams, *J. Am. Chem. Soc., 108* (1986) 40.

5 M. E. Thompson, S. M. Baxter, A. Bulls, B. J. Burger, M. C. Nolan, B. D. Santarsiero, W. P. Shafer and J. E. Bercaw, *J. Am. Chem. Soc., 109* (1987) 203; G. Erker, W. Fromberg, K. Angermund, R. Schlund and C. Krüger, *J. Am. Chem. Soc., 108* (1986) 372.

6 R. F. Jordan, P. K. Bradley, N. C. Baenziger and R. E. LaPointe, *J. Am. Chem. Soc., 112* (1990) 1289.

7 R. J. Goddard, R. Hoffmann and E. D. Jemmis, *J. Am. Chem. Soc., 102* (1980) 7667; F. Volatron and O. Eisenstein, *J. Am. Chem. Soc., 108* (1986) 2173.

8 S. Obara, N. Koga and K. Morokuma, *J. Organomet. Chem., 270* (1984) C33.

9 N. Koga, S. Obara and K. Morokuma, *J. Am. Chem. Soc., 106* (1984) 4625.

10 K. Morokuma, K. Ohta, N. Koga, S. Obara and E. R. Davidson, *Faraday Symp. Chem. Soc., 19* (1984) 49.

11 O. Eisenstein and Y. Jean, *J. Am. Chem. Soc., 107* (1985) 1177.

12 A. Demolliens, Y. Jean and O. Eisenstein, *Organometallics, 5* (1986) 1457.

13 A. Shiga, J. Kojima, T. Sasaki and Y. Kikuzono, *J. Organomet. Chem., 345* (1988) 275.

14 B. E. Bursten and R. H. Cayton, *Organometallics, 5* (1986) 1051.

15 M. J. Calhorda and J. A. M. Simoes, *Organometallics, 6* (1987) 1188.

16 P. Knappe and N. Rösch, *J. Organomet. Chem., 359* (1989) C5.

17 R. L. Williamson and M. B. Hall, *J. Am. Chem. Soc., 110* (1988) 4428.

18 N. J. Fitzpatrick and M. A. McGinn, *J. Chem. Soc., Dalton Trans.*, (1985) 1637; N. Koga and K. Morokuma, *J. Am. Chem. Soc., 110* (1988) 108.

19 M. Brookhart and M. L. H. Green, *J. Organomet. Chem., 250* (1983) 395.

20 L. Versluis, T. Ziegler and L. Fan, *Inorg. Chem., 29* (1990) 4530; L. Versluis and T. Ziegler, *J. Am. Chem. Soc., 112* (1990) 6763; N. Koga, S. Obara, K. Kitaura and K. Morokuma, *J. Am. Chem. Soc., 107* (1985) 7109; D. L. Thorn and R. Hoffmann, *J. Am. Chem. Soc., 100* (1978) 2079; S. Roy, R. J. Puddephatt, and J. D. Scott, *J. Chem. Soc., Dalton Trans.*, (1989) 2121; J. J. Low and W. A. Goddard, *Organometallics, 5* (1986) 609; J. J. Low and W. A. Goddard, *J. Am. Chem. Soc., 108* (1986) 6115; P. K. Byers, A. J. Canty, M. Crespo, R. J. Puddephatt and J. D. Scott, *Organometallics, 7* (1988) 1363.

21 P. Cossee, *J. Catal., 3* (1964) 80; E. J. Arlman, *J. Catal., 3* (1964) 89; E. J. Arlman and P. Cossee, *J. Catal., 3* (1964) 99.

22 K. J. Ivin, J. J. Rooney, C. D. Stewart, M. L. H. Green and R. Mahtab, *J. Chem. Soc., Chem. Commun.*, (1978) 604; M. L. H. Green, *Pure Appl. Chem., 50* (1978) 27.

23 L. Clawson, J. Soto, S. L. Buchwald, M. L. Steigerwald and R. H. Grubbs, *J. Am. Chem. Soc., 107* (1985) 3377.

24 W. E. Piers and J. E. Bercaw, *J. Am. Chem. Soc., 112* (1990) 9406.
25 H. Krauledat and H.-H. Brintzinger, *Angew. Chem., 102* (1990) 1459; *Angew. Chem. Int. Ed. Eng., 29* (1990) 1412.
26 C. A. Jolly and D. S. Marynick, *J. Am. Chem. Soc., 111* (1989) 7968.
27 H. Kawamura-Kuribayashi, N. Koga and K. Morokuma, *J. Am. Chem. Soc., 114* (1992) 2359.
28 M.-H. Prosenc, C. Janiak and H.-H. Brintzinger, *Organometallics, 11* (1992) 4036.
29 B. Rieger and H.-H. Brintzinger, *Angew. Chem.*, in press.
30 L. A. Castonguay and A. K. Rappé, *J. Am. Chem. Soc., 114* (1992) 5832.
31 V. Venditto, G. Guerra, P. Corradini and R. Fusco, *Polymer, 31* (1990) 530; L. Cavallo, G. Guerra, L. Oliva, M. Vacatello and P. Corradini, *Polym. Commun., 30* (1989) 16; P. Corradini, G. Guerra, M. Vacatello and V. Villani, *Gaz. Chim. Ital., 118* (1988) 173.
32 T. A. Albright, J. K. Burdett and M. H. Whangbo, in *Orbital Interactions in Chemistry*, Wiley, New York, 1985, ch. 1 and 2.
33 R. Hoffmann, *J. Chem. Phys., 39* (1963) 1397; R. Hoffmann and W. N. Lipscomb, *J. Chem. Phys., 36* (1962) 2179; *37* (1962) 2872.
34 S. D. Ittel and J. A. Ibers, *Adv. Organomet. Chem., 14* (1976) 33.
35 C. Mealli, and D. M. P. Proserpio *J. Chem. Ed., 67* (1990) 3399.
36 C. Janiak and R. Hoffmann, *Angew. Chem., 101* (1989) 1706; *Angew. Chem. Int. Ed. Engl., 28* (1989) 1688; C. Janiak and R. Hoffmann, *J. Am. Chem. Soc., 112* (1990) 5924.
37 J. H. Ammeter, H.-B. Bürgi, J. C. Thibeault and R. Hoffmann, *J. Am. Chem. Soc., 100* (1978) 3686.
38 K. Tatsumi, A. Nakamura, P. Hofmann, P. Stauffert and R. Hoffmann, *J. Am. Chem. Soc., 107* (1985) 4440.

Appendix

The computations were performed within the Extended Hückel formalism, [33] with weighted H_{ij}'s [37]. The program (ICON) was written and kindly supplied by R. Hoffmann (Cornell University, Ithaca, NY). The atomic parameters for the elements involved in our calculations were as (H_{ii}, ζ): Zr 5s, −9.87 eV, 1.817; 5p −6.76 eV, 1.776; 4d −11.18 eV, 3.835, 1.505 (coefficients for double-ζ expansion: 0.6210, 0.5796) [38]; C 2s, −21.4 eV, 1.625; 2p, −11.4 eV, 1.625 [33]; H 1s, −13.6 eV, 1.3 [33]. Geometrical parameters were fixed as follows: $Zr-C_{alkyl,olefin} = 240$, $Zr-H = 190$, $Zr-C_{Cp} = 250.6$, $(C-C)_{olefin} = 140$, $(C-C)_{ethyl} = 154$, $(C-C)_{Cp} = 141$, $C-H = 110$ pm, Zr–C–H (alkyl) = 112°, C–C–H = 115° (olefin).